Clinical Imaging 55 (2019) 23–28

Contents lists available at ScienceDirect

Clinical Imaging

journal homepage: www.elsevier.com/locate/clinimag

Molecular Imaging and Nuclear Medicine

Improving liver lesion characterisation using retrospective fusion of FDG PET/CT and MRI☆

Arman Parsai[a,b,*], Marc E. Miquel[a,b], Hikmat Jan[a], Adrian Kastler[c], Teresa Szyszko[d], Imene Zerizer[e]

[a] Barts Health NHS Trust, United Kingdom of Great Britain and Northern Ireland
[b] Queen Mary University London, United Kingdom of Great Britain and Northern Ireland
[c] University Joseph Fourier, Grenoble, France
[d] King's College London, United Kingdom of Great Britain and Northern Ireland
[e] Royal Marsden Hospital, United Kingdom of Great Britain and Northern Ireland

ARTICLE INFO

Keywords:
Retrospective
Image fusion
PET/MRI
Focal liver lesion
PET/CT
MRI
FDG

ABSTRACT

Aim: To compare retrospectively fused FDG PET/CT and MRI (PET/MRI) to FDG PET/CT and MRI for characterisation of indeterminate focal liver lesions as malignant or benign in patients with a known primary malignancy.

Materials and method: A retrospective review of 70 patients (30 females, 40 males; mean age 56 ± 14 years) with 150 indeterminate lesions after FDG PET/CT and MRI (mean scan time interval 21 ± 11 days). HERMES® software was used to fuse PET/CT and MRI scans which were reviewed by 2 readers using the Likert score (scale 1–5) to characterise lesions as benign (1–3) or malignant (4–5). Final diagnosis was determined by histopathology or follow up imaging. Results for fused PET/MRI were compared to PET/CT and MRI alone.

Results: For detection, MRI and fused PET/MRI detected all the lesions while PET/CT detected 89.4%. Characterisation of liver lesions as malignant on PET/CT alone yielded sensitivity, specificity, accuracy, PPV and NPV of 55.6%, 83.3%, 66.7%, 83.3%, 55.6% respectively and 67.6%, 92.1%, 80%, 89.3%, 74.5% for MRI, respectively. The sensitivity, specificity, accuracy, PPV and NPV for characterising lesions as malignant increased to 91.9%, 97.4%, 94.7%, 97.1%, 92.5% with PET/MRI fusion. The sensitivity, specificity, accuracy, PPV and NPV of fused PET/MRI for characterising lesions as malignant remained superior to PET/CT and MRI.

Conclusion: Retrospective fusion of PET with MRI has improved characterisation of indeterminate focal liver lesions compared to MRI or FDG PET/CT alone.

1. Introduction

Focal liver lesions are common incidental findings in both asymptomatic patients and those diagnosed with malignancy. The most common malignancies to spread to the liver are colonic, pancreatic, pulmonary and gastric cancers. Patients with colorectal cancer will develop liver metastases during the course of their disease in 50 to 60% of cases [1]. Therefore, accurate imaging of the liver is essential to distinguish benign from malignant lesions, particularly in patients with malignancy in whom early detection and treatment of liver metastases will modify management and influence survival [2]. Currently, ultrasound (US) and computed tomography (CT scan) are used as first line imaging tools to assess liver lesions. Unfortunately, US is operator dependent and of limited diagnostic value if the whole liver cannot be adequately imaged [3]. Dynamic enhanced CT scan has been reported to have higher sensitivity for detecting liver metastases [4,5]. MRI, with its high soft tissue contrast, has been regarded as the best imaging modality for detecting and characterising focal liver lesions [6,7]. However, these modalities rely on differences in tissue properties or differential contrast enhancement to the surrounding normal liver to characterise focal lesions. There is therefore an overlap between benign and malignant liver lesions and some will remain indeterminate even after multimodality imaging. In this situation, invasive assessment with image-guided biopsy and histology is required.

Functional imaging with F18-Fluorodeoxyglucose positron emission tomography and whole body CT (FDG PET/CT) has been reported to be

☆ No conflict of interest to disclose.

* Corresponding author at: The Royal London Hospital NHS Trust, Imaging Department, Whitechapel Road, London E1 1BB, United Kingdom of Great Britain and Northern Ireland.
E-mail address: Arman.Parsai@BartsHealth.nhs.uk (A. Parsai).

https://doi.org/10.1016/j.clinimag.2019.01.018
Received 15 October 2018; Received in revised form 19 January 2019; Accepted 22 January 2019

useful for the detection and depiction of metastatic liver disease and is more accurate for tumour staging [2,8]. Unfortunately, small liver lesions can be missed due to the limited spatial resolution of the PET and the confounding background liver metabolic activity [9].

More recently, integrated PET/MRI systems have been introduced in the research arena but also in particular clinical situations where superior soft tissue resolution is required. Therefore, several authors have successfully assessed the feasibility of combining the PET data with post contrast MRI sequences either retrospectively [10] or prospectively [11]. However, these studies were performed on small selected patient population using only hepatocyte specific contrast (gadolinium-ethoxybenzyl-diethylenetriamine (Gd-EOB-DTPA)). The purpose of this study is to evaluate the feasibility and performance of retrospective fusion of FDG PET/CT and standard MRI sequences using a non-specific extracellular contrast agent (gadoterate meglumine) in detecting and characterising liver lesions in patients with suspected liver metastases.

2. Material and method

This was a retrospective study and received approval at our institution according to the research committee review process.

2.1. Patient selection

70 patients were included in this study (40 males, 30 females; mean age 56 ± 14 years). These were suspected of having malignancy and had at least one indeterminate liver lesion after initial imaging. All patients had half body FDG PET/CT and MRI of the liver with gadolinium (gadoterate meglumine). Imaging was performed at baseline and patients did not have surgery, chemotherapy or radiotherapy 30 days prior to imaging or between FDG PET/CT and MRI scans. A maximum interval of 30 days between MRI and PET/CT was set as an inclusion criterion to avoid appearances of new lesions or changes in characteristics.

2.2. Image acquisition

Gadolinium enhanced MRI and FDG PET/CT studies were acquired separately following a standard protocol. No special sequences or changes in the standard protocol were made to enable the retrospective fusion of PET/CT data with MRI.

2.3. PET/CT

All data were acquired on a Gemini PET/CT system with 3-dimensional time-of-flight (TOF) capability PET scanner together with a 16-slice Brilliance CT scanner (Philips Healthcare, Best, the Netherlands). The patients were asked to follow the standard departmental preparation protocol before the PET/CT according to the European Association of Nuclear Medicine guidelines (EANM) [12]. This included fasting for 4 to 6 h before scanning. The glucose level was assessed before the examination with an acceptable level of < 11 mmol/l [12]. Patients with elevated glucose levels were assessed to find the cause and rescheduled for scanning when the glucose level returned to normal. Scanning started 60 min after injection of 400 (± 10%) MBq (10.8 mCi) of FDG. Patients were imaged supine from skull base to upper thighs with arms raised above head to avoid attenuation artefacts. A low dose CT scan was acquired first (parameters: 40 mAs, 140 kV, 0.5 s per tube rotation) with a slice thickness of 5 mm, a scan length of approximately 900 mm and data acquisition time of 22.5 s. The CT scan was acquired during free breathing. This was immediately followed by PET acquisition with a 3 min per bed position (6–7 bed positions) and 7-slice overlap in 3D reconstruction mode (matrix size 128 × 128). The acquisition time was approximately 30–40 min. The CT data were used for attenuation correction and localization. Iterative reconstruction with ordered-subset expectation maximisation (OSEM) for 3D PET was used to reconstruct the PET raw data. Images were transferred to a HERMES workstation (Hermes Medical Solution, London, UK) for reporting.

2.4. MR imaging

All scans were performed on a 1.5T Achieva system (Philips Healthcare, Best, the Netherlands), in conjunction with a 16-element surface body coil with the surface coil centred on the liver.

Our institutional abdominal MRI protocol for imaging the liver included: coronal T2-weighted turbo spin echo (TSE), axial T2-weighted turbo spin-echo (TSE) with fat suppression (SPAIR), diffusion weighted images, T1-weighted in and opposed phase, and unenhanced and dynamic gadolinium enhanced breathhold T1-weighted images (THRIVE). The dynamic gadolinium enhanced sequences were performed during the hepatic arterial phase (25 s), portal venous phase (70 s) and extracellular phases (at 2 min and 5 min) after intravenous injection of gadoterate meglumine (Dotarem; Guerbet, Villepinte, France) at a dose of 0.2 ml/kg of body weight, as a bolus at a rate of 2 ml/s followed by a 20 ml saline flush. Diffusion weighted images (DWI) were obtained using a free-breathing multi-slice spin-echo echo-planar imaging (EPI) sequence: repetition time (TR) 5300–5800 ms, echo time (TE) 62 ms, EPI factor 60, three averages, field-of-view (FOV) 400–450 mm, rectangular FOV 75%, matrix 112 × 256, 20–28 slices in order to cover the liver, slice thickness 5 mm, slice gap 1 mm. Six motion probing gradients with b-values of 0, 100, 200, 500, 750 and 1000 $s \cdot mm^{-2}$ were applied in three orthogonal directions and trace images were synthesised for each b-value using the mean of three orthogonal directions. ADC maps were calculated on a pixel-by-pixel basis using a mono-exponential fit, and b = 0 was excluded from the calculation in order to eliminate perfusion effects.

2.5. Image registration

Image registration and fusion was performed using the Hermes Gold mediator software (Hermes Medical Solution, London, UK) after importing the MRI data from the PACS using DICOM files format. The software enabled automatic propagation of registration across different series based on 3 methods: automatic, manual and landmark based. In this study, the automatic method corrected manually for any misalignment was used to obtain accurate registration. Both anatomical, contrast enhanced and diffusion weighted MRI sequences (coronal T2-weighted TSE, axial T2-weighted SPAIR, diffusion weighted images, T1-weighted in and opposed phase, and unenhanced and dynamic gadolinium enhanced breathhold T1-weighted images) were retrospectively fused with the corresponding PET component for review.

2.6. Image analysis

All images were reviewed on dedicated workstations. MRI scans were reviewed on the IDS7™ institutional picture archiving and communication system (PACS) workstations (SECTRA, AB, Linköping, Sweden). PET/CT and fused PET/MRI data were interpreted on a HERMES workstation.

The MRI scans, PET/CT and fused PET/MRI images were reviewed by different reader each considered an expert in his/her own field and of a similar level of experience. A gastrointestinal and hepatobiliary radiologist reviewed the MRI scans. A Nuclear Medicine specialist reviewed the PET/CT studies. A dual accredited specialist in nuclear medicine and radiology with current split activity in both specialities reviewed the fused PET/MRI images. All had > 10 years of clinical experience. All readers were blinded to results of other imaging studies, follow-up examinations or biopsy/surgery findings and patient data were reviewed in a random order. The presence, size, location of the liver lesions and corresponding SUVmax were recorded. A 5-point Likert-like scale was used on all modalities according to the likelihood

of malignancy (1, definitely benign; 2, probably benign; 3, indeterminate; 4, probably malignant; 5, definitely malignant). The readers were informed of the scoring system and cut-off values used to reflect the likelihood of malignancy.

2.7. Statistical analysis

Lesion detection was evaluated on MRI, PET/CT and fused PET/MRI regardless of malignancy or benignity of the lesion. Sensitivity, specificity, positive predictive value (PPV) and negative predictive value (NPV) and accuracy in characterising liver lesions were assessed using the Likert score scale. A receiver operating characteristic curve (ROC) was fitted to the reader's confidence in rating the liver lesions. The performance of the three imaging modalities (MRI, PET/CT and fused PET/MRI) was compared using the area under the curve (AUC) given with 1 standard error (± SE) and confidence interval [95% CI].

3. Results

3.1. Patient population

70 patients with suspected malignancy who had whole body FDG PET/CT and MRI of the liver with gadolinium (gadoterate meglumine) were retrospectively included in our study (40 males, 30 females; mean age 56 ± 14 years). A maximum interval of 30 days between these studies was set as an inclusion criterion to avoid appearances of new lesions or changes in characteristics. The mean interval in our cohort was 11 ± 10 days. All patients were imaged at baseline for staging a primary malignancy and did not have surgery, chemotherapy or radiotherapy 30 days prior to imaging or between FDG PET/CT and MRI scans.

3.2. Liver lesions

A total of 150 liver lesions (76 benign; 74 malignant lesions) were present in 70 patients. The lesions remained indeterminate after standard imaging including CT scan and US. The lesions were evenly distributed throughout the liver segments. The number of liver lesions detected and their benign or malignant nature was confirmed either on follow-up imaging (n = 68), histopathology (n = 77) or surgical report (n = 5). Lesions were considered benign if follow-up imaging on CT or MRI demonstrated characteristic imaging features and size was stable for at least 12 months, or if histopathological confirmation was obtained. Lesions were considered malignant if follow-up imaging by CT or MRI demonstrated features more suggestive of malignant disease (increased arterial enhancement, change in morphology consistent with malignancy or increased restriction on DWI) and an increase in size of the lesion over 12 months (RECIST 1.1 criteria), or on histopathology whenever available. All patients had at least one lesion and 4 patients had 2 coexisting lesions (i.e. malignant and benign). The distribution of the different lesions and their SUVmax are given in Table 1 while their size distribution is included in Table 2. A box and whisker plot comparing malignant and benign lesions is shown in Fig. 1.

3.3. Lesion detection

FDG PET/CT detected 134/150 (89.4%) lesions; MRI and fused PET/MRI detected all 150 (100%) lesions. Of the 16 lesions (10.6%) that were not detected by FDG PET/CT 5 (3.3%) were haemangiomas, 6 (6.6%) metastases (5 mucinous adenocarcinoma and 1 neuroendocrine tumour) and 4 (2.6%) HCCs.

3.4. Lesion characterisation

The sensitivity and NPV of FDG PET/CT to characterise lesion as malignant was 55.6%, 57.4% and this increased to 67.6%, 74.5% with MRI and reached 91.9%, 92.5% with PET/MRI, respectively. The false negative (FN) lesions on FDG PET/CT consisted of 2 cholangiocarcinoma, 4 HCCs and 24 metastases. They consisted of 3 HCC and 15 metastases on MRI and 2 HCC, 3 metastasis on PET/MRI. The specificity and PPV of FDG PET/CT alone was lower at 83.3% and 84.2% compared to MRI (92.1%, 89.3%%) and fused PET/MRI (97.4%, 97.1%). The false positive (FP) lesions on FDG PET/CT consisted of 8 abscesses and 4 adenomas. The FP consisted of 9 haemangiomas, 1 hamartomas on MRI and 2 adenomas on PET/MRI. The sensitivity, specificity, accuracy, PPV and NPV for characterising liver lesions as malignant were calculated for FDG PET/CT, MRI and fused PET/MRI by correlating the Likert score given by the readers to the final diagnosis and are

Table 1
Number of lesions, number of patients and SUVmax per lesion patient. (FNH: focal nodular hyperplasia; HCC: hepatocellular carcinoma).

Lesion type		Patients	Lesions	SUVmax
Benign	Abscess	2	8	6.35 ± 2.56
	Adenoma	4	6	2.75 ± 0.64
	Complex Cysts	10	18	2.46 ± 0.40
	FNH	4	8	2.65 ± 0.23
	Haemangioma	16	34	2.23 ± 0.31
	Hamartoma	2	2	1.91 ± 0.18
	Total	38	76	2.80 ± 1.48
Malignant	Cholangiocarcinoma	2	2	2.55 ± 0.19
	HCC	4	6	2.27 ± 0.04
	Metastasis	30	66	6.56 ± 4.27
	Total	36	74	6.16 ± 4.20
Total		70	150	

Table 2
Distribution of lesions according to size.

Distribution	Lesion size (mm)		
	< 10	10 to 20	> 20
Number	28	46	76
Percentage (%)	18.7	30.7	50.7

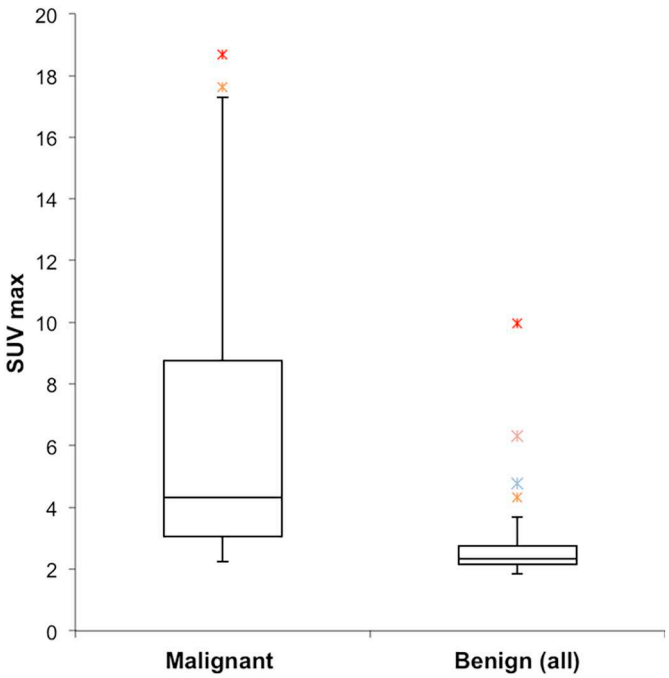

Fig. 1. Box and Whisker plot of the range of SUVmax in benign and malignant liver lesions.

Table 3
Sensitivity, specificity, accuracy, positive and negative predictive values for the different imaging modalities.

Characterisation	Sensitivity (%)	Specificity (%)	Accuracy (%)	PPV (%)	NPV (%)
PET/CT	55.6	83.3	66.7	84.2	57.1
MRI	67.6	92.1	80.0	89.3	74.5
Fused PET/MRI	91.9	97.4	94.7	97.1	92.5

summarised in Table 3. PET/MRI had better sensitivity, specificity, accuracy, positive and negative values compared to MRI and FDG PET/CT for characterising liver lesions as malignant. The ability of the different modalities in characterising liver lesions correctly was assessed using ROC (Fig. 2) and AUC. The AUC for FDG PET/CT was 0.82 ± 0.05 [95% CI 0.72 to 0.92] and 0.92 ± 0.03 [95% CI 0.85 to 0.98] for MRI. The AUC increased to 0.94 ± 0.03 [95% CI 0.9 to 1] using fused PET/MRI.

4. Discussion

FDG PET/CT is widely used for staging cancers and it is becoming a well-established imaging modality in detecting liver metastases. However, studies have shown that MRI has higher sensitivity and specificity for detecting and characterising liver metastases [13]. Moreover, MRI has the ability to characterise and differentiate benign focal liver lesions. Combining both modalities could therefore potentially improve lesion characterisation.

Our results demonstrated a higher detection rate and better characterisation of focal liver lesions as benign or malignant for MRI and fused PET/MRI compared to FDG PET/CT alone. Fused PET/MRI was significantly more sensitive and specific compared to MRI and FDG PET/CT alone in identifying malignant lesions. These results are comparable to previously published studies [10,14]. This is most likely due to the higher soft tissue resolution and enhanced tissue contrast inherent to MRI. The low detection rate of FDG PET/CT was related to lesions not accumulating FDG. They consisted of haemangiomas, mucinous and neuroendocrine liver metastasis and HCC.

For characterising focal liver lesions as malignant, FDG PET/CT had a lower sensitivity, specificity, NPV and PPV compared to MRI or fused PET/MRI. The sensitivity and NPV of FDG PET/CT was 55.6%, 57.4% and this increased to 67.6%, 74.5% with MRI and reached 91.9%, 92.5% with PET/MRI, respectively. The lower sensitivity of FDG PET/CT is partly due the low dose CT protocol used at our institution without intravenous contrast administration and therefore lesions not demonstrating significant FDG accumulation are considered benign. It is well known as mentioned above that some malignant lesions do not demonstrate FDG accumulation such as HCC, hilar cholangiocarcinoma and mucinous metastases. Our results are similar to previously published meta-analyses [10,15], showing FDG PET/CT sensitivity between 61 and 94%. The lower sensitivity of FDG PET/CT in our study is due to the larger cohort of lesions not accumulating FDG compared to the published studies. The sensitivity of MRI and fused PET/MRI was similar to published data. In this study, we found a higher sensitivity and NPV for fused PET/MRI compared to MRI alone for identifying malignant lesions due to the smaller number of false negative lesions. These lesions consisted of poorly differentiated HCC and ocular melanoma metastases. All the lesions accumulated FDG but did not demonstrate the typical enhancement pattern or significant restricted DWI on MRI and therefore were falsely dismissed as hamartomas, atypical haemangiomas and regenerative nodules, respectively (Fig. 3).

The specificity and PPV of FDG PET/CT alone was lower at 83.3% and 84.2% compared to MRI (92.1%, 89.3%%) and fused PET/MRI (97.4%, 97.1%). The higher specificity and PPV for PET/MRI compared to MRI or FDG PET/CT was due to the ability of the fused PET/MRI to correlate the MRI findings with the level of FDG uptake on PET/CT to exclude false positives. These lesions in our cohort included abscesses and adenomas, which are known to accumulate FDG and were therefore falsely diagnosed on PET/CT as malignant lesions while fused PET/MRI images demonstrated the benign characteristics of these lesions. On MRI, atypical haemangiomas, hamartomas were thought to represent malignant lesions, however the fused PET/MRI data showed clearly that these lesions correlated with very low level of FDG uptake confirming their benign nature (Fig. 4).

Overall, the accuracy of fused PET/MRI (94.7%) was superior compared to MRI (80%) or FDG PET/CT (66.7%) alone. Therefore,

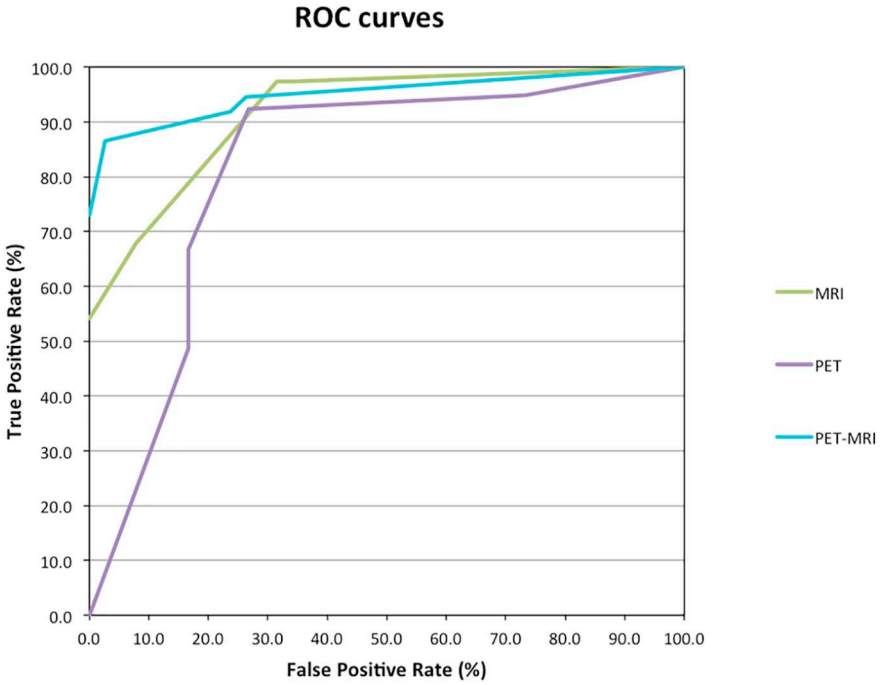

Fig. 2. ROC curves for FDG PET/CT, MRI and PET/MRI.

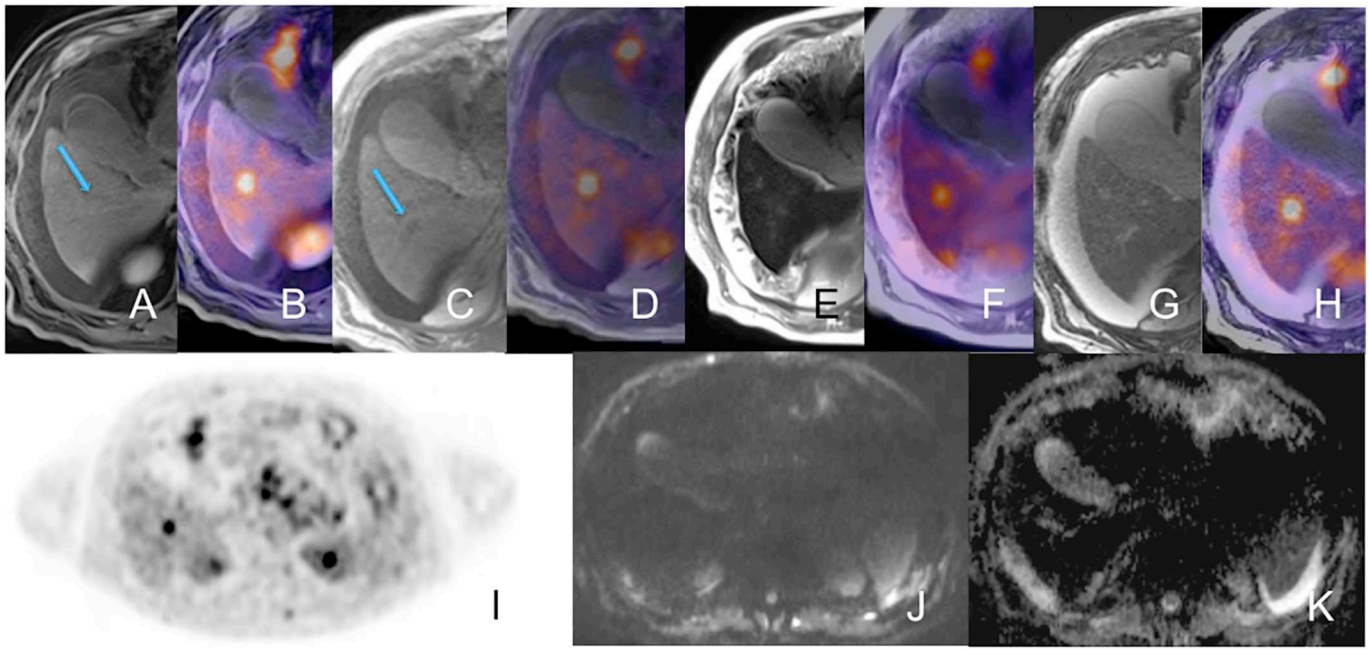

Fig. 3. Ocular melanoma metastasis with lesion in segment VI of the liver characterised as malignant on retrospectively fused PET MRI images but wrongly characterised as benign on MRI. A) T1W fat sat with intravenous gadolinium and C) T1W images demonstrate a low signal lesion (arrow) which was diagnosed as an atypical haemangioma. E) T2 TSE, G) T2 trufi, J) Diffusion Weighted Images at b = 1000 and K) calculated ADC map image did not demonstrate the lesion. The retrospectively fused PET with B) T1W fat sat with intravenous contrast, D) T1W, F) T2 TSE, H) T2 trufi, clearly depict the malignant lesion in segment VI which accumulates FDG. I) PET only image demonstrates accumulation of FDG in the lesion.

combining PET and MRI might be useful for indeterminate lesions after FDG PET/CT and MRI.

The superiority of fused PET/MRI performance in characterising liver lesions was further confirmed on ROC curves and AUC.

Studies have been published on integrated PET/MRI systems for whole body imaging and evaluation of liver lesions. These have found a higher lesion conspicuity and diagnostic confidence for PET/MRI compared to FDG PET/CT [11,16]. However, integrated PET/MRI systems are not widely available and currently expensive. Retrospective fusion of PET and MRI images could be a cost efficient and more widely available alternative to increase diagnostic accuracy. We have demonstrated in our study that this technique is easy to perform and could be

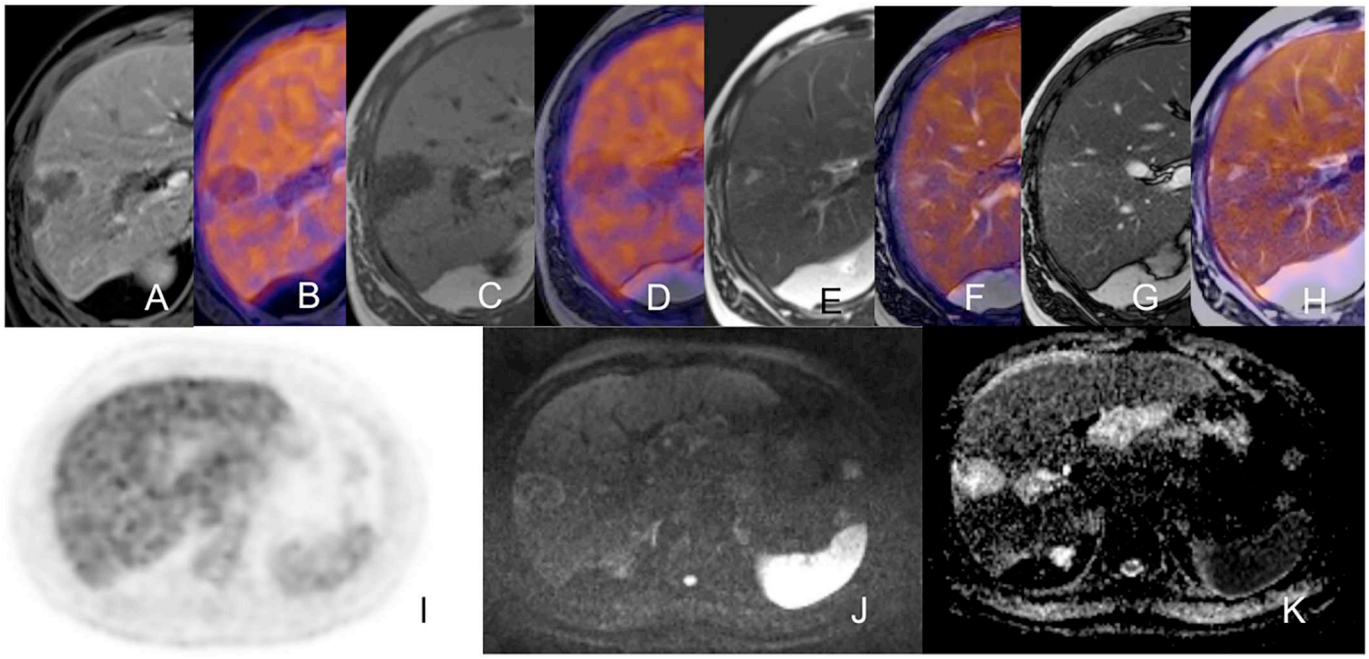

Fig. 4. Atypical partially hyalinised haemangioma in segment VI, which was wrongly characterised as malignant on MRI but properly characterised as benign on retrospectively fused PET MRI images. A) T1W fat sat with intravenous gadolinium demonstrates irregular rim enhancement, C) T1W image demonstrates a low signal lesion, E) T2 TSE and G) T2 trufi demonstrate heterogenous lesion with peripheral low signal changes and central high signal with was diagnosed as central necrosis. J) Diffusion Weighted Images at b = 1000 and K) ADC map demonstrate restriction at the rim of the lesion. I) PET only image demonstrates absence of FDG accumulation in the lesion.

carried out at any centre with PET and MRI scanners. Currently, there are no studies directly comparing the clinical value of retrospective fusion technique to integrated PET/MRI systems for liver lesions and this would be of interest for future studies.

There were a few limitations in our study. Firstly, the FDG PET/CT was obtained with a low dose CT without intravenous contrast administration. Recently, a study [17] has shown improved performance for detection and characterisation of liver lesions using a dual time point acquisition protocol as well as contrast enhanced CT. Secondly, our study consisted of a small cohort of patients which makes statistical analysis less significant. This was partly due to the strict selection criteria with a short interval between the FDG PET/CT and MRI that was set for the study. We continue to collect data for this study and aim at publishing a larger cohort of patients. Thirdly, the retrospective nature of the study resulted in lack of standardisation and therefore differences in protocol acquisition between the MRI and FDG PET/CT. However, despite this limitation we have demonstrated that the fusion technique is feasible and provides good image quality for analysis.

To conclude, our study has demonstrated that retrospective fusion of FDG PET/CT and MRI is a feasible and promising technique in improving detection and characterisation of focal liver lesions, which remain indeterminate after liver MRI and FDG PET/CT.

References

[1] Wiering B, Vogel WV, Ruers TJ, Oyen WJ. Controversies in the management of colorectal liver metastases: role of PET and PET/CT. Dig Surg 2008;25:413–20.

[2] Sacks A, Peller PJ, Surasi DS, Chatburn L, Mercier G, Subramaniam RM. Value of PET/CT in the management of liver metastases, part 1. AJR Am J Roentgenol 2011;197:W256–9.

[3] Parsai A, Zerizer I, Hohmann J, Bongartz G, Beglinger C, Sperandeo G. Remote sonographic interpretation: comparison of standardized video clips to still images. J Clin Ultrasound 2012;40:495–501.

[4] Furuhata T, Okita K, Tsuruma T, Hata F, Kimura Y, Katsuramaki T, et al. Efficacy of SPIO-MR imaging in the diagnosis of liver metastases from colorectal carcinomas. Dig Surg 2003;20:321–5.

[5] Valls C, Andia E, Sanchez A, Guma A, Figueras J, Torras J, et al. Hepatic metastases from colorectal cancer: preoperative detection and assessment of resectability with helical CT. Radiology 2001;218:55–60.

[6] Kinkel K, Lu Y, Both M, Warren RS, Thoeni RF. Detection of hepatic metastases from cancers of the gastrointestinal tract by using noninvasive imaging methods (US, CT, MR imaging, PET): a meta-analysis. Radiology 2002;224:748–56.

[7] Lai DT, Fulham M, Stephen MS, Chu KM, Solomon M, Thompson JF, et al. The role of whole-body positron emission tomography with [18F]fluorodeoxyglucose in identifying operable colorectal cancer metastases to the liver. Arch Surg 1996;131:703–7.

[8] Frankel TL, Gian RK, Jarnagin WR. Preoperative imaging for hepatic resection of colorectal cancer metastasis. J Gastrointest Oncol 2012;3:11–8.

[9] Grassetto G, Fornasiero A, Bonciarelli G, Banti E, Rampin L, Marzola MC, et al. Additional value of FDG-PET/CT in management of “solitary” liver metastases: preliminary results of a prospective multicenter study. Mol Imaging Biol 2010;12:139–44.

[10] Donati OF, Hany TF, Reiner CS, von Schulthess GK, Marincek B, Seifert B, et al. Value of retrospective fusion of PET and MR images in detection of hepatic metastases: comparison with 18F-FDG PET/CT and Gd-EOB-DTPA-enhanced MRI. J Nucl Med 2010;51:692–9.

[11] Beiderwellen K, Gomez B, Buchbender C, Hartung V, Poeppel TD, Nensa F, et al. Depiction and characterization of liver lesions in whole body [(1)(8)F]-FDG PET/MRI. Eur J Radiol 2013;82:e669–75.

[12] Boellaard R, O'Doherty MJ, Weber WA, Mottaghy FM, Lonsdale MN, Stroobants SG, et al. FDG PET and PET/CT: EANM procedure guidelines for tumour PET imaging: version 1.0. Eur J Nucl Med Mol Imaging 2010;37:181–200.

[13] Niekel MC, Bipat S, Stoker J. Diagnostic imaging of colorectal liver metastases with CT, MR imaging, FDG PET, and/or FDG PET/CT: a meta-analysis of prospective studies including patients who have not previously undergone treatment. Radiology 2010;257:674–84.

[14] Coenegrachts K, De Geeter F, ter Beek L, Walgraeve N, Bipat S, Stoker J, et al. Comparison of MRI (including SS SE-EPI and SPIO-enhanced MRI) and FDG-PET/CT for the detection of colorectal liver metastases. Eur Radiol 2009;19:370–9.

[15] Truant S, Huglo D, Hebbar M, Ernst O, Steinling M, Pruvot FR. Prospective evaluation of the impact of [18F]fluoro-2-deoxy-D-glucose positron emission tomography of resectable colorectal liver metastases. Br J Surg 2005;92:362–9.

[16] Rakheja R, Chandarana H, DeMello L, Jackson K, Geppert C, Faul D, et al. Correlation between standardized uptake value and apparent diffusion coefficient of neoplastic lesions evaluated with whole-body simultaneous hybrid PET/MRI. AJR Am J Roentgenol 2013;201:1115–9.

[17] Dirisamer A, Halpern BS, Schima W, Heinisch M, Wolf F, Beheshti M, et al. Dual-time-point FDG-PET/CT for the detection of hepatic metastases. Mol Imaging Biol 2008;10:335–40.